Accelerated Curing of Aryl−Ethynyl End-Capped Polyimide Oligomers and Model Compounds: A Kinetic Study Probing Substituent Effects

Michael E. Wright,*,† Derek A. Schorzman, and Ashley M. Berman

Virginia Commonwealth University, Department of Chemistry, Richmond, Virginia 23284-2006

Received January 29, 2002; Revised Manuscript Received May 16, 2002

ABSTRACT: The compounds *N*-phenyl-4-(10-methoxy-9-anthracenylethynyl)phthalimide (**1**), *N*-phenyl-4-(4-methoxy-1-naphthylethynyl)phthalimide (**2**), and *N*-phenyl-4-(4-benzonitrileethynyl)phthalimide (**3**) were synthesized to probe the effect(s) of electronic subsituents on the thermal curing of aryl−ethynyl end-capped oligomers using end-cap model compounds. The curing kinetics were analyzed using SEC and NMR techniques and Arrhenius parameters were determined and compared to the anthracenyl, naphthyl, and phenyl analogues, **4**, **5**, and **6**, respectively. A thermal curing rate acceleration was attributed to the electron-donating methoxy functionality. This acceleration is independent from the previously observed rate acceleration (phenyl < naphthyl < anthracenyl). Analyses of product distribution of 95% cured model compounds via SEC reveal slight differences between **1** and **4** but no discernible differences between **2** and **5**. The incorporation of the electron-withdrawing group has no effect on the thermal cure rates, as the curing kinetics of **3** are nearly identical to those of **6**. A new end-capping reagent, 4-(4-methoxy-1-naphthylethynyl)phthalic anhydride (**7**) was synthesized and further used in the synthesis of 4-methoxynaphthylethynyl end-capped oligomer (4-MeO−NETI-5). By comparison to NETI-5, no significant changes are introduced by the methoxy- functionality except a reduction in thermal stability via SEC, DSC, and TGA. The curing kinetics of 4-MeO−NETI-5 were determined by monitoring the change in T_g and analysis using the DiBenedetto equation. Unlike all analogous oligomers and model compounds including **2**, a second-order rate law describes the curing kinetics of 4-MeO−NETI-5 better than a first-order rate law. Arrhenius analysis of 4-MeO−NETI-5 using either a first- or second-order rate law results in indistinguishable Arrhenius parameters, and 4-MeO−NETI-5 cures with a lower E_a than NETI-5.

Introduction

In today's world of high energy costs and high tech applications, there continues to be a tremendous need and challenge for the development of lighter and yet mechanically more durable composite materials. One approach that has proven quite successful was initially developed by NASA involving the thermal cure of imide oligomers, which, after curing, affords a final resin with very desirable properties for use in high performance applications.[1−13] Others in the field have explored variations of the phenyl−ethynyl end-capped oligomers as well as probing the mechanism of the curing process(es).[14−24] The phenyl−ethynyl end-capped cured resins in general have shown improved thermooxidative stability and processability over thermally cured acetylene-terminated resins.[25−29] Our research program has built upon the NASA work and developed a variation of the phenyl−ethynyl end-capped oligomers that cure at significantly lower temperatures.[14,19,20] We found that by simply substituting the phenyl moiety with a naphthyl or anthracenyl ring a decrease in curing temperature of 30 and 80 °C, respectively, is observed.

The reactions that lead to the cured resin[10,21] are most likely a variety of cross-linking/chain-extension reactions involving the acetylene moiety.[16,17,21] Although the reaction(s) leading to the cured resin are not fully understood, recent studies of the thermal cure of small compounds that model the end cap have revealed valuable information on the curing process.[10,14,18−21,24] There continues to be a good correlation between the thermal cure kinetics of small model compounds with the kinetic data to the analogous end-capped oligomers;[10,19−21,24] thus, justifying the continued use of model compounds as a tool for probing both the curing mechanism and evaluating potentially useful new end caps.

As mentioned above, we recently reported that the 9-anthracenylethynyl end cap effectively lowers the cure temperature by a remarkable 80 °C. We find it interesting that the rate accelerations shown in our work are not accompanied by any significant changes in the energy of activation (E_a) but, instead, by changes in the Arrhenius parameter (A), which accounts for stereoelectronics, collisional parameters, etc. In one recent study, researchers noted that electron-withdrawing substituents (e.g., imide vs ketone) on the backbone side of the ethynyl unit were found to accelerate thermal curing rates.[15] In addition, data has been presented indicating that electron-withdrawing groups located in the 4-position of the terminal phenyl ring accelerate the curing of imide oligomers.[23] These data, in conjunction with our aryl−ethynyl kinetic data, suggest the importance of stereoelectronic effects in the curing process.

To further study the substituent effects on the aryl−ethynyl systems and to continue our efforts of identifying useful new end-capping reagents, we now report the synthesis and subsequent thermal curing kinetics of naphthyl− and anthracenyl−ethynyl model compounds and analogous oligomers bearing electronically different substituents.

Results and Discussion

Synthesis of Model Compounds and End-Capped Oligomers. The model compounds *N*-phenyl-4-(10-methoxy-9-anthracenylethynyl)phthalimide (**1**), *N*-phenyl-

† Current address: Chemistry & Materials Division, NAWCWD, Code 4T4220D, China Lake, CA 93555.

10.1021/ma020145l CCC: $22.00
Published on Web 07/16/2002

Scheme 1

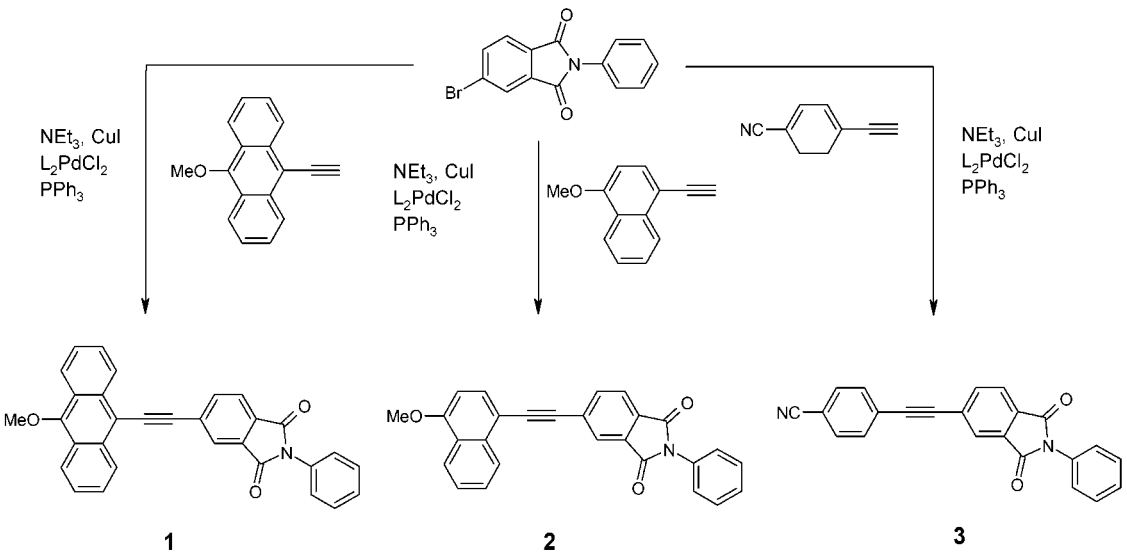

4-(4-methoxy-1-naphthylethynyl)phthalimide (**2**), and *N*-phenyl-4-(4-benzonitrileethynyl)phthalimide (**3**) were synthesized from *N*-phenyl-4-bromophthalimide and the appropriate ethynyl precursor using what are now standard ethynylation techniques (Scheme 1).[14,19,30] The model compounds **1**−**3** are all very soluble in common organic solvents and provide spectroscopic data consistent with the structures drawn in Scheme 1.

To ensure consistency of the current work with previous studies from both our lab as well as others, the curing kinetics of *N*-phenyl-4-(1-anthracenylethynyl)phthalimide (**4**),[14] *N*-phenyl-4-(1-naphthylethynyl)-

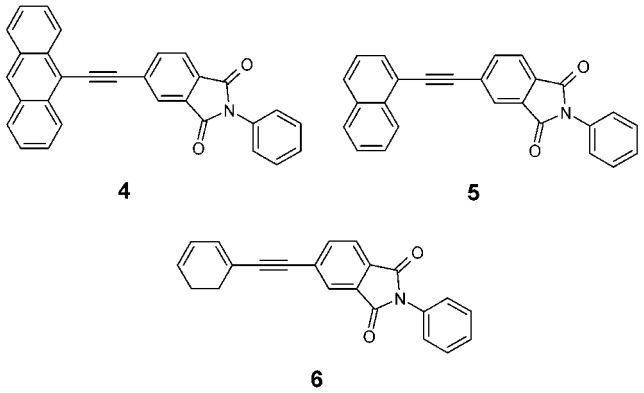

phthalimide (**5**),[19,20] and *N*-phenyl-4-phenylethynylphthalimide (**6**)[14,19−21,24] were carried out concurrently with the new substituted end-cap models **1**−**3**.

The new end-capping reagent, 4-(4-methoxy-1-naphthylethynyl)phthalic anhydride (**7**), is prepared by treating 4-ethynyl-1-methoxynaphthalene with 4-bromophthalic anhydride under standard palladium-catalyzed ethynylation conditions. Compound **7** is then used in the preparation of the 4-methoxy-1-naphthylethynyl-terminated imide oligomer (MeO−NETI-5) using the procedure reported for the synthesis of PETI-5.[12] and naphthyl−ethynyl-terminated imide oligomer (NETI-5).[19] In addition, we report on the synthesis of the bromide end-capped analogue, 4-bromo-terminated imide oligomer (BTI-5). Although not used in the present study, it has tremendous potential for the creation of reactive end caps placed in position after imidization or used in the synthesis of block copolymers via catalytic cross-coupling methodology.

Thermal Curing of Model Compounds 1−6. In a similar manner, as we reported previously, a series of neat samples of each model compound were sealed under nitrogen atmosphere in glass ampules and uniformly heated for varying time periods at various temperatures ranging from 250 to 350 °C in a calibrated aluminum heating block.[14,19,20] Thermal curing of all model compounds in the solvent-free melt was performed to recreate the thermal curing conditions of the analogous oligomers. Following thermal curing, the sample vials were removed via suction and the cured samples were further analyzed. The new model compounds **1**−**3** exhibited complete solubility before and after thermal curing in THF at concentrations sufficient for analysis by SEC.[14] In the case of model compound **2**, very good solubility in $CDCl_3$ before and after curing made kinetic analysis by proton NMR spectroscopy possible[19,20] in addition to analysis by SEC. Progress of the reaction is monitored by measuring the concentration of the unreacted arylethynyl−imide at selected times. This is accomplished by using peak integration and comparison to the normalized trace (SEC analysis) or the use of an internal NMR standard, 1,2-dichloroethane.

The curing kinetics for the new compounds (**1**−**3**) and previous compounds (**4**-**6**)[14,19,20] are best described by a *pseudo*-first order rate law. The slight overlapping of peaks in the SEC traces inherently introduces error into each sample. However, a comparison of R^2 values from linear regression calculations using first and second order rate laws consistently indicates that a first-order rate law describes the experimental data better than second order at all temperatures. The experimental rate data is evaluated in an Arrhenius analysis (i.e. $1/T$ vs ln k) and is presented in Figure 1. Further analysis of data provides the Arrhenius parameters that are summarized in Table 1.

Arrhenius analysis of **1**, **2**, **4**, and **5** revealed a rate acceleration attributed to the methoxy functionality, as **1** and **2** cure significantly faster than **4** and **5**, respectively, at each temperature. The faster rates are not accompanied by a reduction in E_a values; the E_a values of **1**, **2**, and the reference compound **5** are statistically

Table 1. Arrhenius Parameters as Calculated from Experimental Rate Data Using SEC Analysis[b]

sample	**1**	**2**	**3**	**4**[14]	**5**[19]	**6**[a]
R^2	0.971776	0.989121	0.980833	0.997553	0.993 33	0.987886
E_a (kJ/mol)	146(25)	158(17)	178(25)	119(6)	172(14)	181(18)
A (min^{-}1)	4×10^{13}	1×10^{15}	4×10^{13}	3×10^{9}	6×10^{13}	8×10^{16}

[a] Model compound **6** was reevaluated for heating block calibration purposes. The new values are reported and are in good agreement with previous values.[14,19] [b] The numbers in parentheses represent the error in the last digit(s).

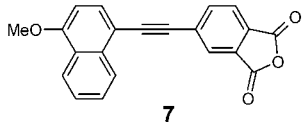

7

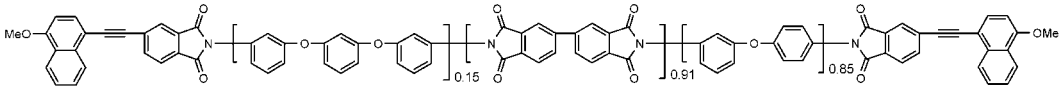

MeO-NETI-5

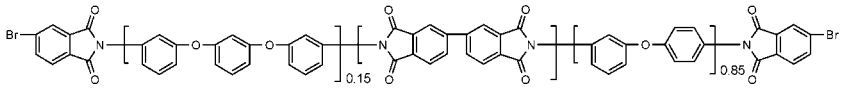

BTI-5

indistinguishable from each other. In addition to the rate acceleration provided by the methoxy functionality, **1** cures faster than **2** at all temperatures, establishing the apparent independence of the acceleration provided by the aromatic ring from the electron-donating substituent. Additionally, kinetic analysis of **2** using NMR is in good agreement with kinetic analysis using SEC as demonstrated by the similar experimental rate values using each method. A correlation between kinetic analyses using NMR and SEC was previously noted for model compounds **5** and **6**.[19]

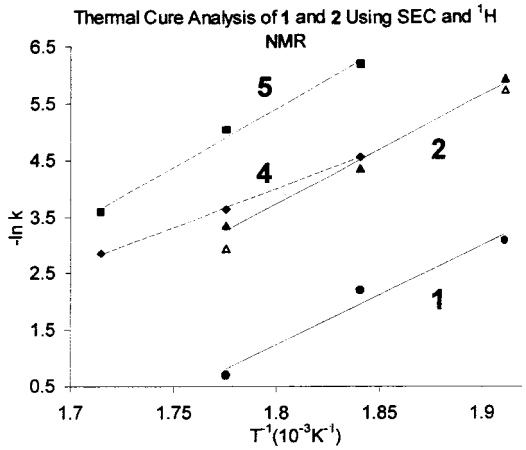

Figure 1. Arrhenius analysis of the thermal curing kinetics of model compounds **1** (●), **2** (▲), **4** (♦),[14] and **5** (■).[14,19] Solid data points were collected using SEC analysis. Hollow data points were collected using ^{1}H NMR analysis. Linear regressions were calculated from SEC data only. Solid line represents new data; dashed line represents previously reported data.[14,19]

Using the experimental kinetic data, model compounds **1**, **2**, **4**, and **5** were cured at sufficient temperature and time necessary for ~95% cure completion. The cured materials are dissolved in THF and analyzed by SEC analysis. The latter SEC traces of the cured products are plotted alongside the SEC trace of the uncured material (Figure 2). The expanded traces reveal only slight changes in the product peaks over the 40 °C temperature range used. In addition, the product peaks of different model compounds are remarkably similar to each other, although one difference is noteworthy. Product traces of **1** and **4** appear to have slight shoulders, on the higher MW side of the major peak for **1**, on the lower MW side for **4.** This indicates a slight change in product distribution due to the presence of the electron-donating group. Model compounds **2** and **5**, however, both demonstrate nearly identical cured peaks, suggesting very similar product distribution.

A very interesting comparison of cure data is summarized in Figure 3. Arrhenius analysis of **3** reveals no significant change in the curing kinetics due to the electron-withdrawing cyano functionality. The experimental Arrhenius parameters of **3** and **6** are not just statistically indistinguishable, but nearly identical. There are some indications that electron-withdrawing groups (e.g. CF_3) have accelerated the curing of imide oligomers;[23] however, our data might suggest that the acceleration is perhaps due to some secondary process involving the chemistry of the electron-withdrawing group (EWG) itself and not the ethynyl linkage.

Analysis of End-Capped Oligomers. SEC analyses of the new oligomers, MeO−NETI-5, and BTI-5 were performed by dilution in THF (2 mg/mL) and then injection onto a Hewlett-Packard 1100 HPLC/SEC system. Molecular weights in this study are reported relative to polystyrene standards. The experimental values of M_w and PD of MeO−NETI-5 were found to correlate well with NETI-5 (Table 2).[19]

Analyses of the oligomers using TGA were performed using a Perkin-Elmer TGA-7. To ensure standardized drying, each sample was first heated to 250 °C at a rate of 20 °C/min under a nitrogen atmosphere with a flow rate of 20 cm^3/min and immediately cooled. Data were then collected up to 700 °C at a rate of 20 °C/min with a nitrogen flow of 20 cm^3/min. Analysis of the previously synthesized PETI-5 and NETI-5 indicates similar thermal degradation (Figure 4). Onset of weight loss occurs at approximately 510 °C and becomes rapid by approximately 600 °C for both NETI-5 and PETI-5. This indicates that the naphthyl moiety does not introduce

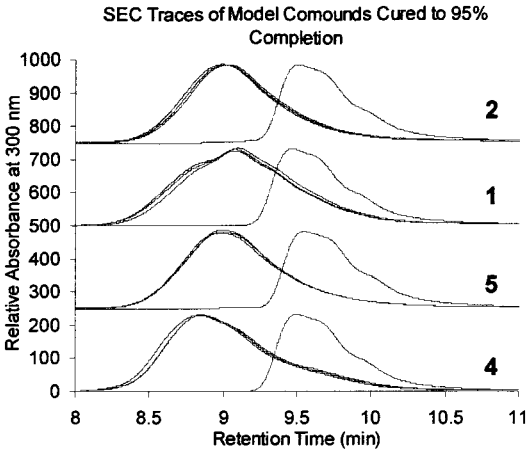

Figure 2. SEC traces of uncured (higher retention time) and cured **1**, **2**, **4**, and **5**. Cured traces include data from 95% curing at all temperatures used in kinetic analysis (**1** and **2**, 250, 270, and 290 °C; **4** and **5**, 270, 290, and 310 °C).

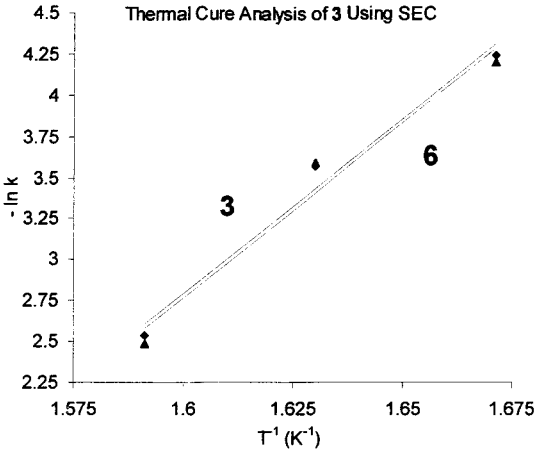

Figure 3. Arrhenius analysis of the thermal curing kinetics of **3** (♦) and **6** (▲) from kinetic data collected using SEC analysis. Linear regression lines are shown. Model compound **6** was reevaluated for heating block calibration purposes.

Table 2. SEC and DSC Data for Oligomers MeO−NETI-5 and NETI-5[19]

sample	NETI-5[19]	MeO−NETI-5
M_n (g/mol)	2213	2384
PD	1.83	2.38
T_m (°C)	266.4	220.2
T_{gu} (°C)	231.6	199.8
T_{gc} (°C)	266.5	272.1

a significant decrease in thermal stability. Analysis of MeO−NETI-5 does indicate a decrease in thermal stability (Figure 5). Onset of weight loss occurs at approximately 410 °C and continues slowly and steadily until approximately 550 °C, when rapid decomposition begins. The slow first stage of thermal decomposition of MeO−NETI-5 is most likely due to decomposition of the methoxy functionality. Further weight loss, however, does appear to roughly correspond to NETI-5.

Analyses of MeO−NETI-5 using DSC were performed using a Perkin-Elmer DSC-7 at a rate of 20 °C/min under nitrogen at a flow rate of 20 cm^3/min. The first scan revealed a broad melting peak (T_m) at 220.2 °C. After the sample was allowed to cool, the second scan revealed a well-defined uncured glass transition (T_{gu}) at 199.8 °C (Figure 6). The sample was next thermally cured using the standard conditions of 380 °C for 1 h. A third scan revealed a fully cured glass transition (T_{gc})

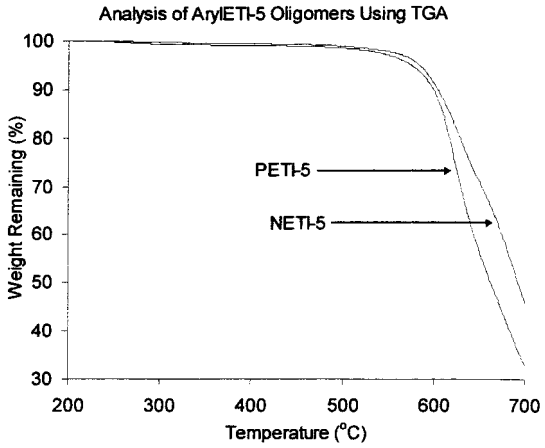

Figure 4. TGA traces of arylETI-5 oligomers.

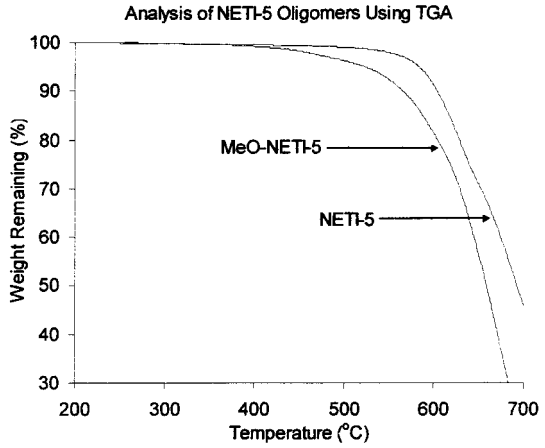

Figure 5. TGA traces of NETI-5 oligomers.

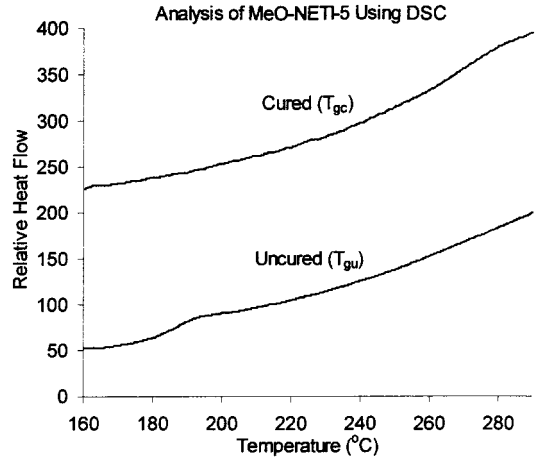

Figure 6. Traces of uncured (bottom) and fully cured (top) DSC scans of MeO−NETI-5.

at 272.1 °C. Although the T_{gu} of MeO−NETI-5 is somewhat lower than NETI-5, the T_{gc} value is reasonably close. These data suggest that the two final resins are very similar in structure.

Thermal Cure Analysis of End-Capped Oligomers. Neat samples of MeO−NETI-5 were sealed and cured as described above. Analyses of the thermal curing of the end-capped oligomers were performed by monitoring the change in T_g as a function of time using the DiBenedetto equation,[31−34] modified for highly cross-linked networks

$$(T_g - T_{gu})/(T_{gc} - T_{gu}) = \lambda x/(1 - (1 - \lambda)x)$$

where T_g, T_{gu}, T_{gc}, λ, and x represent the glass transition temperature of the sample, the glass transition temperature of the uncured material, the glass transition temperature of the fully cured material, the ratio of the isobaric heat capacity of fully cured model compound to that of uncured model compound, and the reaction extent (e.g., $C_t/C_0 = 1 - x$), respectively. The experimental values of T_{gu} and T_{gc} listed in Table 1 were used in the calculation of reaction extent for each oligomer. The previously determined value of λ for PETI-5 ($\lambda = 0.69$),[21] which has been successfully applied to other slightly modified PETI-5 systems,[14,19] was used in the calculations.

Applying a first-order rate law (e.g. $\ln[C_t/C_0]$ vs time) to MeO−NETI-5 revealed an apparent systematic deviation from linearity. Instead, a second-order rate law (e.g. $1/[C_t/C_0]$) was found to describe the reaction much more accurately. This was found to be true at all three temperatures at which MeO−NETI-5 was cured, one of which is shown (Figure 7).

This is the first example of direct contradiction between model compound and analogous oligomer kinetics out of the many systems we have studied. Either the dilution of end caps in the oligomer melt reveals a mechanism that is occurring, but undetectable in **4**, or the thermal cure of **4** reacts with a different mechanism than the analogous end-capped oligomer MeO−NETI-5.

Using the experimental rate data, an Arrhenius plot was constructed (Figure 8). It is interesting to note that regardless of the choice of rate law (first or second order) the same Arrhenius parameters are calculated within experimental error for MeO−NETI-5 and previously collected NETI-5[19] data (Table 3). This justifies the comparison of E_a and A values for the two oligomers, despite the potentially different mechanisms. MeO−NETI-5 is found to cure with significantly faster rates than NETI-5 at the temperatures studied, with a significantly lower E_a.

Concluding Remarks

The synthesis of model compounds bearing electronic substituents was accomplished and the thermal curing kinetics were analyzed using established techniques. We consistently observe first-order rate laws for all model compounds at all temperatures. The kinetic data for the model compounds show that the electron-donating methoxy substituent accelerates the curing process, and as before, the change is with based on the Arrhenius constant and not the energy of activation. Analyses of the cured model compounds by SEC indicate little or no dependence of product size distribution on curing temperature. There does appear to be some small changes in the cured products for the anthracenyl model (MeO− vs H); however, the overall product distribution appears very similar in all model compounds studied to date. It was interesting to find that the electron-withdrawing cyano substituent had no measurable effect on the curing reaction.

The new MeO−NETI-5 oligomer was prepared and characterized by TGA analysis and indicates a slightly lower degradation temperature of approximately 400 °C than PETI-5 or NETI-5, presumably due to the degradation of the methoxy functionality. The curing kinetics of MeO−NETI-5 reveal the expected increase in cure rate at a given temperature; however, the methoxy group promotes a mechanistic change in the curing of the polymer. MeO−NETI-5 clearly demonstrates second-order kinetics, whereas, the thermal cure of NETI-5 is best described by first-order kinetics. This is the first example where we have observed a rate law change in going from the model compound to the analogous oligomer. On a final note, regardless of the choice of rate law, or the driving force behind the rate acceleration (entropy vs enthalpy), the model studies once again proved to be valuable in predicting cure rates for the oligomers. This intriguing change in rate law warrants further investigation as well as a full analysis of the mechanical properties of these new, fast curing imide oligomers.

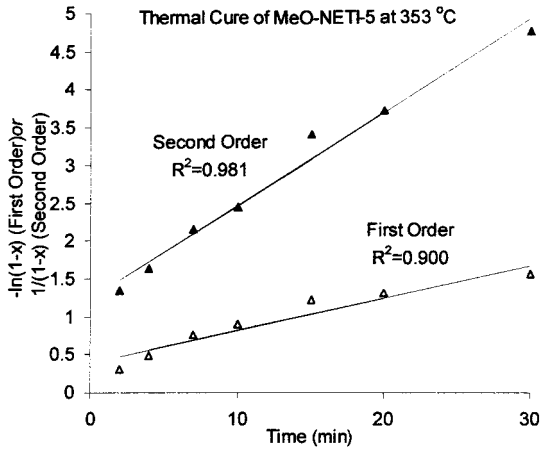

Figure 7. Reaction profile of MeO−NETI-5 using DSC and DiBenedetto analysis. Data analysis using first order (hollow) and second order (solid) rate laws are shown with linear regression and R^2 values.

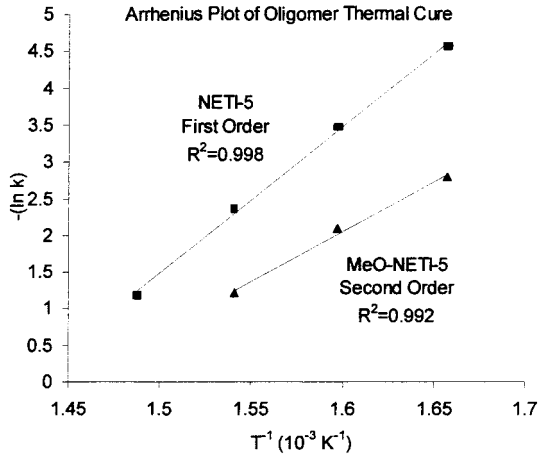

Figure 8. Arrhenius analysis of oligomer thermal curing kinetics using DSC. NETI-5[19] (■) was calculated using first-order rate data and methoxy-NETI-5 (▲) was calculated using second-order rate data. Linear regression data is also included.

Table 3. Arrhenius Parameters Calculated for NETI-5[19] and MeO−NETI-5 Rate Data Calculated Using First- and Second-Order Rate Laws[a]

	NETI-5[19]		MeO−NETI-5	
	first order[19]	second order	first order	second order
R^2	0.997 94	0.997 94	0.974499	0.991928
E_a (kJ/mol)	165.3(53)	165.3(53)	115.0(186)	113.0(102)
A (min^{-1})	2.0×10^{12}	2.0×10^{12}	1.9×10^{8}	3.6×10^{8}

[a] Numbers in parentheses represent error in last significant digits.

Experimental Section

General Methods. All manipulations of compounds and solvents were done under nitrogen using standard Schlenk line techniques. Triethylamine (CaH_2) and THF (Na^0) were purified from were purified by distillation under nitrogen from the specified drying agents. ^1H NMR and ^{13}C NMR measurements were performed on either a Varian Mercury 300 MHz or a Varian Inova 400 MHz instrument. ^1H NMR and ^{13}C NMR chemical shifts are reported vs the respective solvent residue peak (^1H, ^{13}C: solvent = $CDCl_3$, δ 7.25 ppm, δ 76.9 ppm; solvent DMSO-d_6, δ 2.62 ppm, δ 36.9 ppm). The compounds 4-ethynylbenzonitrile,[35] 4-bromo-1-methoxynaphthalene,[36] and 9-bromo-1-methoxyanthracene[37] were prepared according to literature techniques. The compounds 4-bromobenzonitrile, 1-methoxynaphthalene, anthrone, 3,4′-oxydianiline, and 3,3′,4,4′-biphenyltetracarboxylic dianhydride were purchased from Aldrich Chemical Co. The compounds 1,3-bis(3-aminophenoxy-)benzene and 4,4′-oxydiphthalic anhydride were purchased from TCI America and trimethylsilylacetylene was purchased from GFS Chemicals, Inc. SEC analyses were performed by dilution in THF (2 mg/mL) and then injection onto a Hewlett-Packard 1100 HPLC (column: PL 300 × 7.5 mm, 5 μm particle size). Molecular weights are calculated relative to polystyrene standards. TGA analyses were performed using a Perkin-El mer TGA-7 at 20 °C/min heating rate under 20 cm^3/min nitrogen flow. DSC analyses were performed using a Perkin-Elmer DSC-7 at 20 °C/min heating rate under 20 cm^3/min nitrogen flow. Elemental analyses were performed at Atlantic Microlab Inc., Norcross, GA.

Synthesis of *N*-Phenyl-4-(10-methoxy-9-anthracenylethynyl)phthalimide (1). To a solution of 9-bromo-1-methoxyanthracene (0.58 g, 2.0 mmol), triphenylphosphine (50 mg,0.19 mmoL), copper iodide (20 mg, 0.11 mmoL), and palladium bis(triphenylphosphine) dichloride (30 mg, 0.04 mmoL) in triethylamine (10 mL) was added trimethylsilylacetylene (0.43 mL, 3.0 mmoL), and the mixture was heated for 1 h at reflux. The cooled mixture was diluted with ether (75 mL) and filtered. The solution was washed with H_2O (3 × 75 mL), dried over Na_2SO_4, filtered, and solvents were removed under reduced pressure to yield crude 9-trimethylsilylacetylene-1-methoxyanthracene. The crude product was diluted in methanol (75 mL), 3.5 M $KOH_{(aq)}$ (0.5 mL) was added, and stirred vigorously for 1 h. The mixture was quenched with H_2O (75 mL) and extracted with hexane (3 × 75 mL). The organic was dried over Na_2SO_4 and filtered, and solvents were removed under reduced pressure to yield 9-ethynyl-1-methoxyanthracene (0.20 g, 43.1%) that was used without further purification. A solution of *N*-phenyl-4-bromophthalimide (0.33 g, 1.09 mmol), triphenylphosphine (30 mg, 0.11 mmol), copper iodide (10 mg, 0.53 mmol), and palladiumbistriphenylphosphine dichloride (15 mg, 0.21 mmol) in triethylamine (5 mL) was treated with a solution of crude 9-methoxy-1-anthracenylacetylene (0.38 g, 1.63 mmol) in benzene (5 mL) and the mixture was heated at reflux for 1 h. The cooled solution was diluted in dichloromethane (200 mL), washed with H_2O (3 × 150 mL), dried over Na_2SO_4, and filtered, and the solvents were removed under reduced pressure. Recrystallization from toluene afforded *N*-phenyl-4-(9-methoxy-1-anthracenylethynyl)phthalimide (0.31 g, 62.7%) as a brick red solid. ^1H NMR ($CDCl_3$): δ 4.19 (s, 3 H), 7.43−7.69 (m, 9 H), 7.99 (d, J = 7.8 Hz, 1 H), 8.09 (d, J = 7.8 Hz, 1 H), 8.26 (s, 1 H), 8.36 (d, J = 8.4 Hz, 2 H), 8.63 (d, J = 8.7 Hz, 2 H). ^{13}C NMR ($CDCl_3$): δ 63.6, 91.4, 98.3, 111.6, 122.7, 123.7, 124.2, 125.6, 126.1, 126.4, 126.5, 127.2, 128.0, 129.0, 129.9, 130.2, 131.4, 132.0, 133.8, 136.6, 154.3, 166.5. Mp 260−265 °C. Anal. Calcd for $C_{31}H_{19}NO_3$: C, 82.10; H, 4.22. Found: C, 81.35; H, 4.42.

Synthesis of 4-Ethynyl-1-methoxynaphthalene. To a solution of 4-bromo-1-methoxynaphthalene (1.18 g, 4.98 mmol), triphenylphosphine (130 mg, 0.50 mmoL), copper iodide (50 mg, 0.26 mmoL), and palladium bis(triphenylphosphine) dichloride (70 mg, 0.10 mmoL) in triethylamine (10 mL) was added trimethylsilylacetylene (1.1 mL, 7.78 mmoL), and the mixture was heated for 1 h at reflux. The cooled mixture was diluted with ether (75 mL) and filtered. The solution was washed with H_2O (3 × 75 mL), dried over Na_2SO_4, filtered, and solvents were removed under reduced pressure to yield crude 4-trimethylsilylacetylene-1-methoxynaphthalene. The crude product was diluted in methanol (50 mL), 3.5 M KOH(aq) (0.5 mL) was added, and the reaction was stirred vigorously for 1 h. The mixture was quenched with H_2O (50 mL) and extracted with hexane (2 × 75 mL). The organic was dried over Na_2SO_4 and filtered, and solvents were removed under reduced pressure to yield 4-ethynyl-1-methoxynaphthalene (0.88 g, 97.0%), which was used without further purification: ^1H NMR ($CDCl_3$): δ 3.59 (s, 1 H), 3.96 (s, 3 H), 6.71 (d, J = 8.1 Hz, 1 H), 7.58 (t, J = 7.6 Hz, 1 H), 7.67 (t, J = 7.6 Hz, 1 H), 7.73 (d, J = 8.1 Hz, 1 H), 8.59 (d, J = 8.0 Hz, 1 H), 8.41 (d, J = 8.3 Hz, 1 H). ^{13}C NMR ($CDCl_3$): δ 55.3, 103.1, 111.5, 122.0, 124.9, 125.5, 125.5, 127.1, 131.6, 134.1155.9.

Synthesis of *N*-Phenyl-4-(4-methoxy-1-naphthylethynyl)phthalimide (2). A mixture of *N*-phenyl-4-bromophthalimide (0.99 g, 3.3 mmol), triphenylphosphine (90 mg, 0.34 mmol), palladium bis(triphenylphosphine) dichloride (50 mg, 0.07 mmol), and copper iodide (30 mg, 0.16 mmol) in triethylamine (10 mL) was treated with a solution of crude 4-ethynyl-1-methoxynaphthalene (0.88 g, 4.83 mmol) in benzene (10 mL), and the resulting mixture was heated at reflux for 2 h. The cooled mixture was diluted in dichloromethane (150 mL), washed with H_2O (3 × 100 mL), dried over Na_2SO_4, and filtered, and the solvents were removed under reduced pressure. Recrystallization from toluene yielded *N*-phenyl-4-(4-methoxy-1-naphthylethynyl)phthalimide (0.78 g, 58.6%) as a yellow solid. ^1H NMR ($CDCl_3$): δ 4.04 (s, 3 H), 6.83 (d, J = 8.1 Hz, 1 H), 7.41−7.58 (m, 6 H), 7.66 (t, J = 7.4 Hz, 1 H), 7.75 (d, J = 8.1 Hz, 1 H), 7.91−7.97 (m, 2 H), 8.13 (s, 1 H), 8.32 (t, J = 9.3 Hz, 2 H). ^{13}C NMR ($CDCl_3$): δ 55.7, 91.3, 93.1, 103.5, 111.5, 122.3, 123.6, 125.2, 125.4, 125.8, 126.1, 126.3, 127.5, 128.0, 128.9, 129.7, 130.4, 131.4, 131.9, 133.9, 136.6, 156.7, 166.5. Mp 227−231 °C. Anal. Calcd for $C_{27}H_{17}NO_3$: C, 80.38; H, 4.25. Found: C, 80.11; H, 4.44.

Synthesis of *N*-Phenyl-4-(4-cyanophenylethynyl)phthalimide (3). A mixture of 4-(*N*-phenyl)-bromophthalimide (0.89 g, 2.9 mmol), cuprous iodide (0.04 g, 0.21 mmol), triphenylphosphine (0.08 g, 0.32 mmol), and bis(triphenylphosphine)palladium dichloride (0.04 g, 0.06 mmol) in triethylamine (25 mL) was treated with a solution of 4-ethynylbenzonitrile (0.72 g, 5.7 mmol) in benzene (10 mL) and heated for 1 h at reflux. The cooled reaction mixture was diluted in dichloromethane (150 mL) and washed with H_2O (3 × 100 mL); the organic layer was dried over Na_2SO_4 and decanted, and solvents were removed under reduced pressure. The crude product was recrystallized from toluene and dried at reduced pressure to afford *N*-phenyl-4-(1-benzonitrileethynyl)phthalimide as a light tan solid (0.66 g, 64.5%). ^1H NMR ($CDCl_3$, 400 MHz): δ 7.39−7.45 (m, 3 H), 7.50−7.54 (m, 2 H), 7.64−7.70 (m, 4 H), 7.92 (d, J = 7.6 Hz, 1 H), 7.97 (d, J = 7.6 Hz, 1 H), 8.09 (s, 1 H). ^{13}C NMR ($CDCl_3$, 400 MHz): δ 91.3, 91.8, 112.5, 118.1, 123.8, 126.4, 126.7, 126.8, 128.2, 128.7, 129.1, 131.1, 131.3, 132.0, 132.1, 132.3, 137.4, 166.3, 166.4. Mp 290−292 °C. Anal. Calcd for $C_{23}H_{12}N_2O_2$: C, 79.30; H, 3.47. Found: C, 78.36; H, 3.52.

Synthesis of 4-(4-Methoxy-1-naphthylethynyl)phthalic Anhydride (7). A mixture of 4-bromophthalic anhydride (1.32 g, 5.8 mmol), palladium bis(triphenylphosphine) dichloride (82 mg, 0.17 mmol), copper iodide (55 mg, 0.29 mmol), and triphenylphosphine (0.15 g, 0.58 mmol) in triethylamine (10 mL) was treated with a solution of 4-methoxy-1-naphthylacetylene (1.59 g, 8.73 mmol) in benzene (10 mL) and heated for 1 h at reflux. The cooled mixture was filtered, and the precipitate was added to $NaHCO_3$(aq). (0.5 M, 100 mL) and allowed to react for 1 h with vigorous stirring. The mixture was diluted with acetone (125 mL) and filtered. The precipitate was added to toluene (100 mL), and the mixture was heated for 1 h at reflux. The cooled mixture was filtered, washed with toluene (3 × 10 mL), and dried under reduced pressure affording 4-(4-methoxy-1-naphthylethynyl)phthalic anhydride (0.92 g, 48.3%) as a bright yellow powder. ^1H NMR (DMSO-d_6): δ 4.17 (s, 3 H), 7.23 (d, J = 8.1 Hz, 1 H), 7.76 (t, J = 7.5 Hz, 1 H), 7.86 (t, J = 7.7 Hz, 1 H), 8.03 (d, J = 8.1 Hz, 1 H),

8.25 (d, $J = 7.8$ Hz, 1 H), 8.33−8.38 (m, 2 H), 8.51−8.57 (m, 2 H). Anal. Calcd for $C_{21}H_{12}O_4$: C, 76.82; H, 3.68. Found: C, 76.70; H, 3.67.

Synthesis of 4-(4-Methoxy-1-naphthyl)ethynyl-Terminated Imide Oligomer (MeO−NETI-5). A solution of 1,3-bis(3-aminophenoxy)benzene (0.19 g, 0.66 mmol), and 3,4′-oxydianiline (0.75 g, 3.7 mmol) in *N*-methylpyrollidinone (35 mL) was treated with 4-(4-methoxy-1-naphthyl)ethynyl anhydride (0.26 g, 0.79 mmol) and 3,3′,4,4′-biphenyltetracarboxylic anhydride (1.17 g, 4.00 mmol), and the solution was allowed to react 15 h under nitrogen at ambient temperature. The solution was diluted with toluene (100 mL), the reaction vessel was equipped with a Dean−Stark trap, and the mixture was heated at reflux 15 h. The cooled solution was added to H_2O (150 mL), stirred vigorously 30 min, and filtered. The filtrate was washed successively with H_2O (3 × 15 mL) and warm methanol (3 × 15 mL) and was dried under reduced pressure and 85 °C 15 h to afford 4-(4-methoxy-1-naphthyl)ethynyl-terminated imide oligomer (0.88 g, 38%): $M_n = 2152$; PD = 2.38.

Synthesis of 4-Bromine Terminated Imide Oligomer (BTI-5). A solution of 1,3-bis(3-aminophenoxy)benzene (0.19 g, 0.66 mmol) and 3,4′-oxydianiline (0.75 g, 3.7 mmol) in *N*-methylpyrollidinone (35 mL) was treated with 4-bromophthalic anhydride (0.18 g, 0.79 mmol) and 3,3′,4,4′-biphenyltetracarboxylic anhydride (1.18 g, 4.00 mmol), and the solution was allowed to react for 15 h under nitrogen at ambient temperature. The solution was diluted with toluene (100 mL), the reaction vessel was equipped with a Dean−Stark trap, and the mixture was heated at reflux 15 h. The cooled solution was added to H_2O (150 mL), stirred vigorously 30 min, and filtered. The filtrate was washed successively with H_2O (3 × 15 mL) and warm methanol (3 × 15 mL) and was dried under reduced pressure and 85 °C 15 h to afford the 4-bromine terminated imide oligomer (0.92 g, 41%): $M_n = 1965$; PD = 2.65.

Acknowledgment. The authors are grateful to the Office of Naval Research for partial funding of this work. D.A.S. would like to acknowledge the Office of Graduate Studies at Virginia Commonwealth University for support through the graduate research fellowship award. A.M.B. would like to acknowledge the Department of Chemistry at Virginia Commonwealth University and the National Science Foundation for funding through the Research Experience for Undergraduates (REU) program. We would also like to extend our thanks to the Mary Kapp Fund for partial support of this work and the purchase of the 300 MHz NMR spectrometer.

References and Notes

(1) Chang, A. C.; Jensen, B. J. *J. Adhes.* **2000**, *72*, 209−217.
(2) Connell, J. W.; Smith Jr., J. G.; Hergenrother, P. M.; Rommel, M. L. *High Perform. Polym.* **2000**, *12*, 323−333.
(3) Connell, J. W.; Smith Jr., J. G.; Hergenrother, P. M. *J. Macromol. Sci., Rev. Macromol. Phys.* **2000**, *C40*, 207−230.
(4) Hergenrother, P. M.; Connell, J. W.; Smith Jr., J. G. *Polymer* **2000**, *41*, 5073−5081.
(5) Hinkley, J. A.; Proctor, D. A. *J. Adv. Mater.* **2000**, *32*, 35−41.
(6) Smith Jr., J. G.; Connell, J. W. *High Perform. Polym.* **2000**, *12*, 213−223.
(7) Smith Jr., J. G.; Connell, J. W.; Hergenrother, P. M. *J. Compos. Mater.* **2000**, *34*, 614−627.
(8) Preston, C. M. L.; Hill, D. J. T.; Pomery, P. J.; Whittaker, A. K.; Jensen, B. J. *High Perform. Polym.* **1999**, *11*, 453−465.
(9) Connell, J. W.; Smith Jr., J. G.; Hergenrother, P. M. *High Perform. Polym.* **1998**, *10*, 273−283.
(10) Hinkley, J. A. *J. Adv. Mater.* **1996**, *27*, 55−59.
(11) Hergenrother, P. M.; Bryant, R. G.; Jensen, B. J.; Havens, S. J. *J. Polym. Sci., Part A: Polym. Chem.* **1994**, *32*, 3061−3067.
(12) Hergenrother, P. M.; Smith Jr., J. G. *Polymer* **1994**, *35*, 4857−4864.
(13) Jensen, B. J.; Hergenrother, P. M. *J. Macromol. Sci. Pure Appl. Chem.* **1993**, *A30*, 449−458.
(14) Wright, M. E.; Schorzman, D. A. *Macromolecules* **2001**, *34*, 4768−4773.
(15) Ayambem, A.; Mecham, S. J.; Sun, Y.; Glass, T. E.; McGrath, J. E. *Polymer* **2000**, *41*, 5109−5124.
(16) Cho, D.; Drzal, L. T. *J. Appl. Polym. Sci.* **2000**, *76*, 190−200.
(17) Fang, X.; Xie, X. Q.; Simone, C. D.; Stevens, M. P.; Scola, D. A. *Macromolecules* **2000**, *33*, 1671−1681.
(18) Holland, T. V.; Glass, T. E.; McGrath, J. E. *Polymer* **2000**, *41*, 4965−4990.
(19) Wright, M. E.; Schorzman, D. A.; Pence, L. E. *Macromolecules* **2000**, *33*, 8611−8617.
(20) Wright, M. E.; Schorzman, D. A. *Macromolecules* **1999**, *32*, 8693−8694.
(21) Fang, X.; Rogers, D. F.; Scola, D. A.; Stevens, M. P. *J. Polym. Sci., Part A: Polym. Chem.* **1998**, *36*, 461−470.
(22) Jayaraman, S.; Srinivasan, R.; McGrath, J. E. *J. Polym. Sci., Part A: Polym. Chem.* **1995**, *33*, 1551−1563.
(23) Johnston, J. A.; Li, F. M.; Harris, F. W.; Takekoshi, T. *Polymer* **1994**, *35*, 4865−4873.
(24) Takekoshi, T.; Terry, J. M. *Polymer* **1994**, *35*, 4874−4880.
(25) Douglas, W. E.; Overend, A. S. *Eur. Polym. J.* **1993**, *29*, 1513−1519.
(26) Sastri, S. B.; Keller, T. M.; Jones, K. M.; Armistead, J. P. *Macromolecules* **1993**, *26*, 6171−6174.
(27) Swanson, S. A.; Fleming, W. W.; Hofer, D. C. *Macromolecules* **1992**, *25*, 582−587.
(28) Lucotte, G.; Cormier, L.; Delfort, B. *J. Polym. Sci., Part A: Polym. Chem.* **1991**, *29*, 897−903.
(29) Sefcik, M. D.; Stejskal, E. O.; McKay, R. A.; Schaefer, J. *Macromolecules* **1979**, *12*, 423−425.
(30) Neenan, T. X.; Whitesides, G. M. *J. Org. Chem.* **1988**, *53*, 2489−2496.
(31) Hale, A.; Macosko, C. W.; Bair, H. E. *Macromolecules* **1991**, *24*, 2610−2621.
(32) Pascault, J. P.; Williams, R. J. J. *J. Polym. Sci., Part B: Polym. Phys.* **1990**, *28*, 85−95.
(33) Couchman, P. R. *Macromolecules* **1987**, *20*, 1712−1717.
(34) DiBenedetto, A. T. *J. Polym. Sci., Part B: Polym. Phys.* **1987**, *25*, 1949−1969.
(35) Takahashi, S.; Kuroyama, Y.; Sonogashira, K.; Hagihara, N. *Synthesis* **1980**, *8*, 627−630.
(36) Carreno, M. C.; Garcia Ruano, J. L.; Sanz, G.; Toledo, M. A.; Urbano, A. *J. Org. Chem.* **1995**, *60*, 5328−5331.
(37) Meyer II, K.; Schlosser, H. *Justus Liebigs Ann. Chem.* **1920**, *420*, 126−133.

MA020145L